On the Extendibility of X-ray Crystallography to Noncrystals

D. Sayre,*† H. N. Chapman‡ and J. Miao

Department of Physics, SUNY, Stony Brook, NY 11794, USA. E-mail: sayre@bnl.gov

Abstract

This paper discusses the concept that crystallinity is not an essential requirement for applying the techniques of X-ray crystal structure analysis. Assuming this to be true, the removal of crystallinity as a prerequisite for the techniques would allow the imaging of structures well beyond the present range of sizes accessible to X-ray crystallography. An example of an imageable structure could be a single small biological cell, containing perhaps 10^{13}–10^{14} Da. The proposed concept differs from the usual diffraction method of studying noncrystalline structure, *i.e.* small-angle scattering, in carrying out the diffraction experiment and subsequent processing as if the structure being studied were in fact the asymmetric unit of a crystal: *i.e.* orienting the structure in all directions in the X-ray beam needed to explore its Fourier transform (F transform), and phasing and inverting the transform to obtain the electron-density image of the structure. The one actual difference from the crystal case is that the F transform is faint and also continuous, rather than displaying discrete intense Bragg spots. As a result, to get a readable pattern, the structure must be exposed to high levels of radiation. This last fact creates the principal limitation of the technique. With single air-dried biological cells at room temperature as diffracting specimens and soft X-rays in the wavelength range 18–32 Å, patterns to date have not been observed beyond resolutions of 140–300 Å before radiation damage has become evident. At this resolution, the technique nevertheless would lie on the same curve of resolution *vs* specimen size as do the existing major imaging techniques of X-ray crystallography, electron microscopy and light microscopy, falling directly between the latter two. Thus, X-ray diffractive imaging is not destroyed by the withdrawal of crystallinity but instead is shifted to a new size range of structures, which have hitherto been somewhat inaccessible to imaging. A method for phasing the diffraction pattern, based on the ability to sample the pattern more finely than in the case of the crystalline specimen, is giving good results in preliminary testing. The principal need at present is for better instrumentation for collecting the diffraction data, including the additional motions needed for collecting data in three dimensions.

† Mailing address: 15 Jefferson Court, Bridgewater, NJ 08807, USA.
‡ Present address: Advanced Microtechnology Program, Lawrence Livermore National Laboratory, Livermore, CA 94551, USA.

1. Introduction

The thought that crystallinity (or near-crystallinity as in powder or fiber diffraction) may not be essential to the application of the techniques of crystal structure analysis while on reflection not surprising appears to have been first suggested in a paper by Sayre (1980). In the years since then, the subject has gradually progressed (Sayre *et al.*, 1984; Yun *et al.*, 1987; Sayre, 1991; Sayre & Chapman, 1995) to the point where it is now considerably more than a concept only, the two critical steps in the procedure (observation of the diffraction patterns generated and phasing) having now been shown separately to be capable of being carried out. At the same time, the complete procedure has not yet been carried out in any one instance, so that a full description of the procedure is not yet feasible. In these circumstances, it seems desirable to summarize the position that the subject has reached today.

2. Observing the diffraction pattern

2.1. *Illuminating the specimen*

All our work to date has been carried out with bending-magnet soft X-rays or undulator X-rays, produced at the X-ray synchrotron facility at Brookhaven National Laboratory (Rarback *et al.*, 1990). This type of source is excellent in terms of (*a*) giving copious X-rays, (*b*) allowing beamline processing to good monochromaticity and photon parallelism at the specimen, and (*c*) good tunability over a range of X-ray wavelengths potentially highly useful in this form of structure imaging. This is not to say that other sources (normal laboratory or X-ray laser) or shorter wavelengths [see in particular the parenthetical remark given in (*c*) of Note 2 of Sayre & Chapman (1995)] may not be useful also, but that the synchrotron sources, except for their comparative rarity, are indeed excellent for this application, lacking only (*d*) the perhaps useful ability of providing intense X-ray pulses of very short duration. Fortunately, synchrotron sources are increasingly coming on line at a number of locations (Winick, 1994).

Notes on the above: Item (*a*) is desirable because of the faintness of the diffraction pattern. (*b*) is needed to create a sharp sphere of reflection, which in turn is needed to avoid blurring and consequent loss of detail in the continuous diffraction pattern (Sayre *et al.*, 1988). (*c*)

arises because, throughout the wavelength range concerned, the behavior of atomic scattering factors in the vicinity of absorption edges depends strongly on the chemical species and on the chemical state. The result is that a technique that can produce electron-density maps at selected wavelengths in this range can not only map structure but can indicate chemistry as well (see §4). (d) is mentioned because of its stop-motion capabilities and because of its potential ability to capture a diffraction pattern before the full effects of radiation damage have developed.

Following monochromatization by a grating in the beamline, photon parallelism at the specimen has been secured in all our work to date by placing a small pinhole (typically 15 µm in diameter) a few centimeters upstream of the specimen; the angular spread of photons reaching the specimen is then no greater than the angular size of the pinhole as viewed from the specimen. This technique has not been very successful and probably should be abandoned; it places a large amount of strongly illuminated scattering material (the material at the pinhole edge) too near the specimen itself, so that the detector really records the sum of two scattering experiments, one on the specimen and one on the pinhole edge. We have combated this situation by adding further screening of the detector in various ways that take advantage of the difference in position of the pinhole and specimen, but at the cost of adding still more unwanted material near the specimen and a more complicated alignment procedure. Rather than using that method, we would now advocate having as little extraneous material as possible in the vicinity of the specimen, and obtaining the photon parallelism with a low-numerical-aperture focusing element (zone plate or mirror) located well upstream from the specimen.

2.2. Mounting the specimen

Throughout our work, we have mounted specimens on ultrathin membranes as supplied for use in electron microscopy or on silicon nitride membranes as widely used in work with soft X-rays. (*Warning*: it appears that minute defects with considerable diffracting power can appear in silicon nitride membranes.) An alternative mounting technique might be on a microfiber or micropipette or in a microcapillary, which would keep the amount of extraneous material in the X-ray beam more nearly constant during the required changes in specimen orientation in three-dimensional work (see *Remarks on the diffraction geometry* below).

2.3. Positioning the specimen

Placing and centering the micrometer-size specimen in the few-micrometer-size beam has been another problem that we have not solved in a really convenient way in most of our work to date. Our approach has been based on introducing a small piece of radiachromic film [film

impregnated with a dye that changes color on exposure to X-rays, see Guttmann *et al.* (1988)] to mark the beam position, placing the cross-hairs of an optical microscope on the radiachromic film spot, and then bringing the specimen onto the cross-hairs with a manual x, y positioning stage. Unfortunately, the components have not been of quite the necessary precision; also, an additional problem has been introduced by our general apparatus design, which requires that the system be evacuated part way through the above steps, allowing the vacuum forces to disturb the positioning slightly. The result has been that getting a good picture has often been a matter of luck rather than certainty. The problem is not a fundamental one, however, and will be corrected in our next design.

2.4. Detecting the pattern

Most of our work to date has been carried out using special soft-X-ray-sensitive silver halide film (Kodak type XUV-T100, no longer available) as a detector. This is an excellent film, with good detective quantum efficiency for soft X-rays and a fine grain, the latter allowing a short specimen-to-film distance (1 in in most of our work); patterns are then viewed under a low-power microscope. However, offsetting these qualities is the 15 min processing delay in seeing the result of an exposure and the fact that our stock is old and has a considerable sprinkling of fog grains, rendering faint pattern hard to see, and reducing the detective quantum efficiency (DQE) considerably. For this reason, we have begun using a back-thinned charge-coupled device (CCD) as detector, operating it in direct soft-X-ray mode (no fluorescent screen) and at a larger distance from the specimen (typically 5–10 in) because of its lower spatial resolution. Our tentative conclusion is that its immediate viewing and inherent digitalization will make it a more satisfactory detector overall.

2.5. Examples of observed pattern

In the years of this work, we have made hundreds of exposures, resulting in many dozens of recorded patterns, out of which there are five groups of patterns for which we can state with near-certainty the identity of the object giving rise to the pattern. Examples of these five groups, plus an example of the type of pattern arising from minute defects in some of the membranes we have used for specimen mounting, are shown in Fig. 1. In all five groups, there has been repeated observation of the pattern, with independent information supporting the genuineness of the pattern also present in the cases of Figs. 1(a), (b) and (c). Fig. 1(d) shows the pattern from a material whose diffraction extends to the highest resolution found in the five groups and Fig. 1(e) shows the type of pattern perhaps best characterizing the average generic type of biological cell. [Specimens (b)–(d) are each of specialized type.] In our view, the
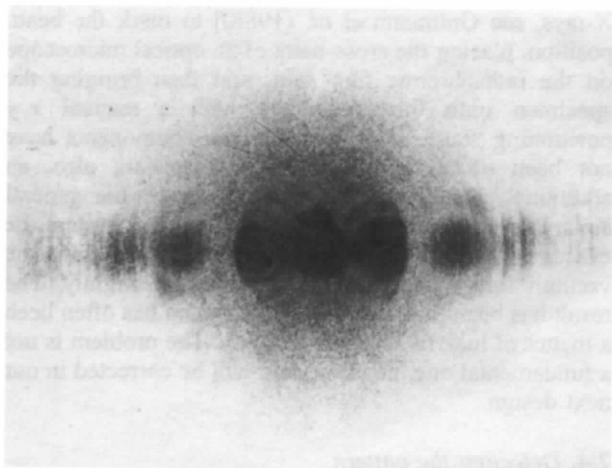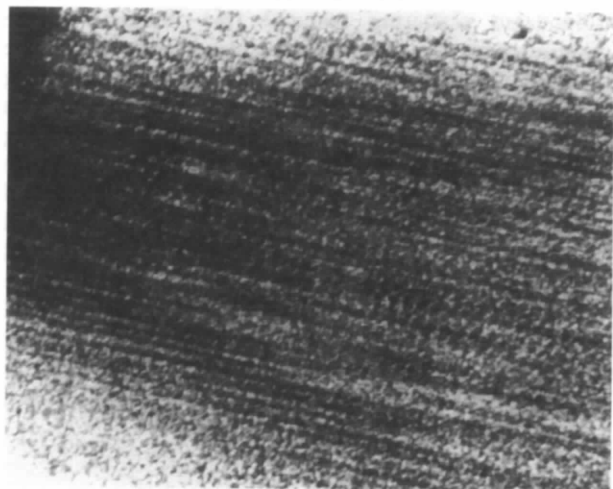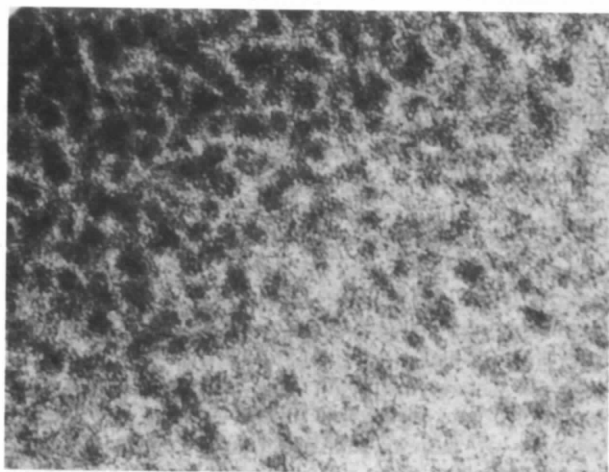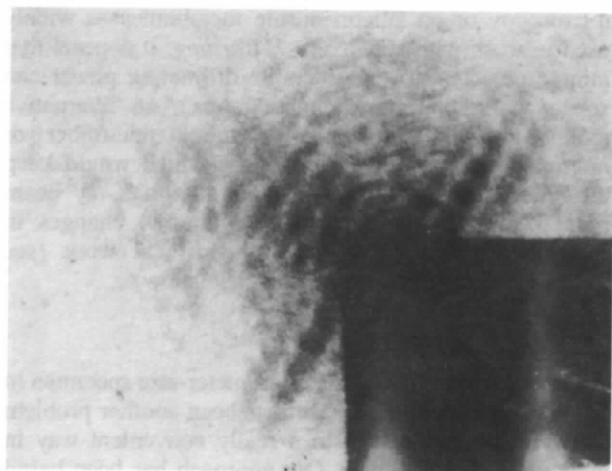
(a)
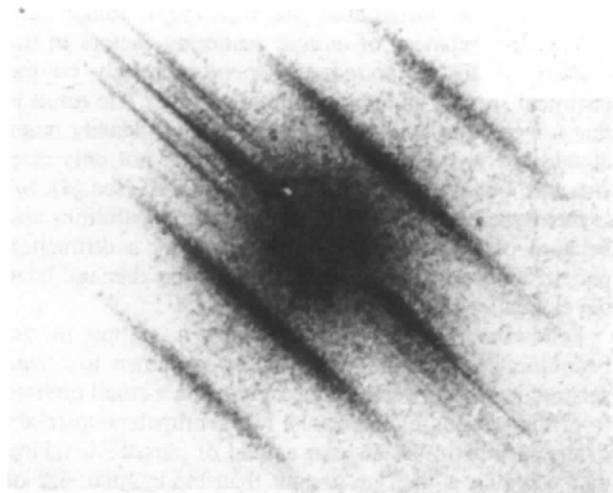
(b)
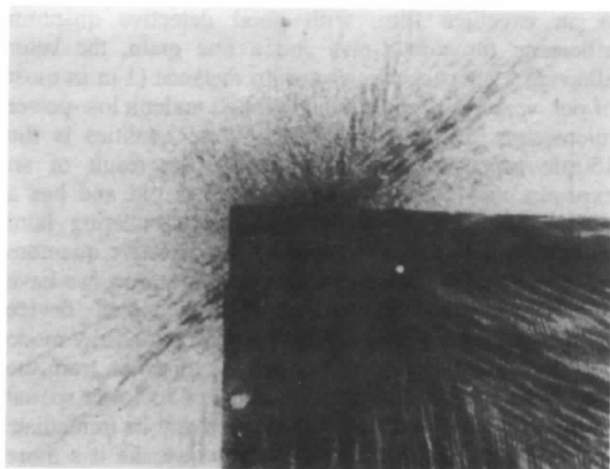
(c)

(d)

(e)

(f)

examples shown are sufficient to establish the observability of the F transform intensity of individual micrometer-size noncrystalline biological objects, even with techniques that are less than optimal. For comparison, Fig. 2 shows the computed diffraction pattern corresponding to Fig. 1(a).

As will be noted from these examples, in the newer work (Figs. 1a, c, d, e), patterns have been observed to resolutions of approximately 140–300 Å; specimen sizes in this work have been typically 2–3 μm. Fig. 3 shows this point on a plot of resolution vs specimen size, together with the corresponding points for the standard imaging techniques (X-ray crystallography, electron microscopy and light microscopy) when applied to complex biological material. It is seen that all four techniques lie on a common curve, thus justifying the view that loss of crystallinity does not destroy X-ray analysis but rather shifts it to a new size range of structures. For theoretical arguments that explain why the two X-ray techniques fall approximately where they do on this curve, see Figs. 5 and 3 of Sayre & Chapman (1995). This work, we believe, correctly replaces our earlier more optimistic estimates of achievable resolution based on simple wavelength considerations (Yun et al., 1987) and on illumination coherence (Sayre, 1991). However, it should be noted that the older estimates could again take on meaning if e.g. cryogenic techniques of protecting specimens against radiation damage should prove strongly effective.

2.6. The transition to three-dimensional work

To date, all work has been with one beam direction, monochromatic X-rays, and the specimen stationary; i.e. all of the exposure that the specimen has undergone has been devoted to studying the intersection of the F transform of the specimen with a single stationary sphere of reflection. For future three-dimensional work, this exposure will have to be distributed over a multiplicity of positions of the reflecting sphere and it is to be expected that the imaging resolution will suffer. A very rough estimate of this can be made but is unsubstantiated as yet by any direct data. Assuming that several hundred
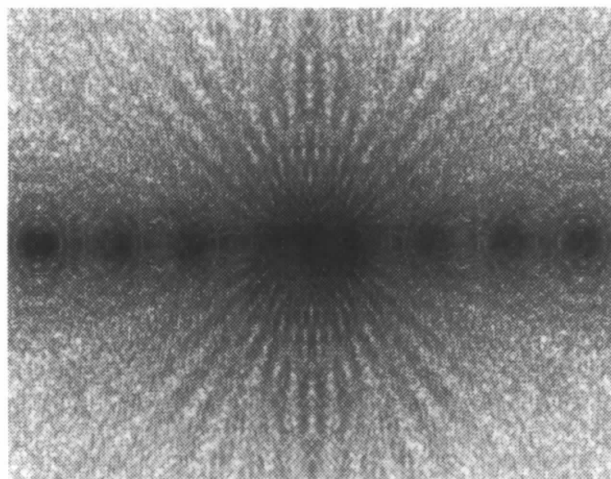

Fig. 2. Computed diffraction pattern corresponding to Fig. 1(a). The agreement is good enough to establish the pattern authenticity, but is clearly not exact, probably due mainly to simplifying assumptions made in this figure concerning the specimen illumination, where a small circular portion of zone plate was assumed to be uniformly illuminated, while the actual illumination in Fig. 1(a) was more complex (i.e. pinhole Airy pattern plus unwanted scattering from the pinhole edge material).
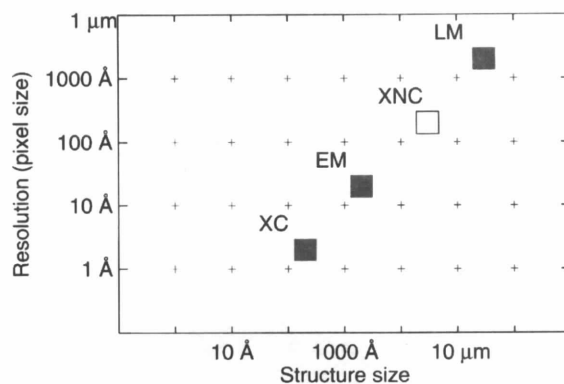

Fig. 3. Imaging resolution vs specimen size. Typical values are shown by solid squares for the major techniques for imaging internal structure in biological materials (XC = X-ray crystallography, EM = electron microscopy, LM = light microscopy). The position expected for the X-ray noncrystal technique (= XNC) discussed in this paper is shown by the open square.

Fig. 1. Examples of recorded diffraction patterns. (a) Pattern from a small portion of a Fresnel zone plate. The zone plate was of the type used to focus X-rays in a scanning X-ray microscope. Exposure 5 s, wavelength 18 Å, pattern extends to about 200 Å resolution. For comparison, the expected pattern, as calculated on a computer, is shown in Fig. 2. (b) A diatom (air-dried, unknown species). Exposure 30 min, wavelength 32 Å, pattern extends to about 400 Å resolution. From Yun et al. (1987). (c) Bull sperm tail (air-dried, specimen courtesy R. Balhorn and N. Hud). Exposure 15 min, wavelength 18 Å, pattern extends to about 300 Å resolution. The dark quadrant in the lower right arises from a technique of placing the specimen near a corner of the boundary frame of the specimen-supporting membrane to screen 270° of the photograph from pinhole-edge scattering [used also in (a), (d) and (f)]. The darkness of that quadrant gives an idea of the strength of the pinhole-edge scattering. (d) Single myofibril of honeybee flight muscle (air-dried, specimen courtesy S. F. Fan and Y. Yeh). The origin is off the picture to the upper left. Exposure 5 min, wavelength 27 Å, pattern extends to about 250 Å. With 2.5 h exposure at 18 Å wavelength, the pattern extends to about 140 Å resolution. (e) Minutocellus polymorphis (marine phytoplankton) (air-dried, specimen courtesy Center for Culture of Marine Phytoplankton, West Boothbay Harbor, Maine). The origin is off the picture to the upper left. Exposure 20 min, wavelength 18 Å, pattern extends to about 300 Å resolution. From Sayre (1991). (f) A minute defect on a silicon nitride membrane. Exposure 11 min, wavelength 25.7 Å, pattern extends to about 500 Å resolution. All exposures employed undulator radiation except for (b), which used bending-magnet radiation. Patterns are shown highly enlarged with the film graininess visible in most cases. The full pattern extent is not shown in some cases.

orientations of the specimen will be needed for three-dimensional work, this would mean a decrease of 2.5 orders of magnitude in the exposure that could be allotted to a single exposure or a worsening by 1/8 that amount [in view of the eighth-power law relating dosage to resolution found by Sayre & Chapman (1995)] or about 0.3 of an order of magnitude, or factor of 2, in the expected resolution. Assuming cooling of the specimen to cryogenic temperatures and the replacement of our noisy film detector by a CCD, at least an order of magnitude in terms of exposure should be regained, reducing the factor in terms of resolution to approximately 1.5. The uncertainty here is probably the greatest present uncertainty concerning the technique.
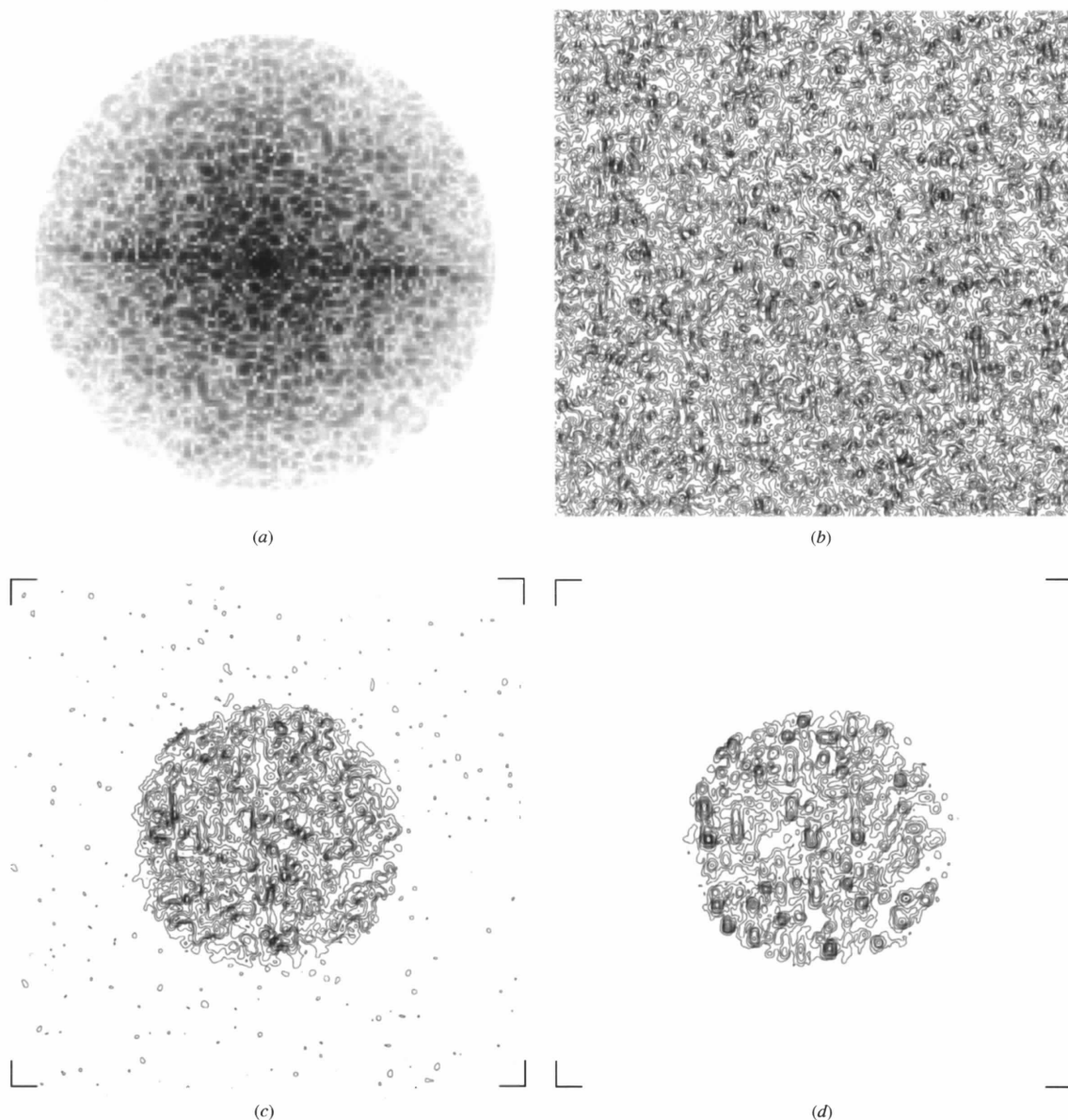

(a)   (b)

(c)   (d)

Fig. 4. An example of phasing by oversampling. (a) The 2× oversampled data set of 13 965 magnitudes submitted to the phasing algorithm. In order to accommodate the dynamic range in the printing process, a few strong terms near the origin were driven to saturation. (b)–(e) The maps of the structure found by the phasing algorithm after 0, 50, 100 and 200 phasing cycles. The action of the phasing in confining the scattering density to the circular envelope can be followed. The time spent in reaching (e) was 5 min on an IBM RISC 6000 computer. (f) The map made with the known correct phases. (g), (h) Similar to (e), (f), except that 17% (peak-to-peak) random noise was added to the data-set magnitudes to simulate experimental error, and that (g) shows the map after 425 phasing cycles. (g) shows slight effects of the noise, as does (h), although at a lower contour level than is shown here. All maps give the magnitude of the complex scattering density. The density is actually real in (f), however, and very nearly real in (e), (g) and (h).

2.7. Remarks on the diffraction geometry and on the overall pattern

Some aspects of the diffraction geometry, as it arises in the technique under discussion, may be noted. The reflecting sphere, at the soft-X-ray wavelengths that we have used, has a radius typically some 20 times smaller than in X-ray crystallography. At the same time, and in keeping with the much lower resolutions observed, the observable diffraction patterns extend only to distances from the origin of reciprocal space some 100 times smaller than in X-ray macromolecular crystallography, with most of the observable pattern lying closer to the origin than do even the lowest-order Bragg reflections in the macromolecular crystal case.

A result of this is that diffraction in the noncrystal case is confined to fairly small scattering angles even with soft X-rays, typically about a tenth of a radian. This in turn has an advantage, namely that in three-dimensional work rotation of the specimen about a single axis misses only a small fraction of the observable data, and even that small fraction can be observed by simply tilting the axis by a few degrees and repeating a few degrees of the rotation scan. The result is that, with a fiber, micropipette or capillary support, the quantity of material supporting the specimen can be kept nearly constant in the X-ray beam during a three-dimensional diffraction experiment, a matter of importance in maintaining data-set accuracy in view of the small volume of the specimen itself.
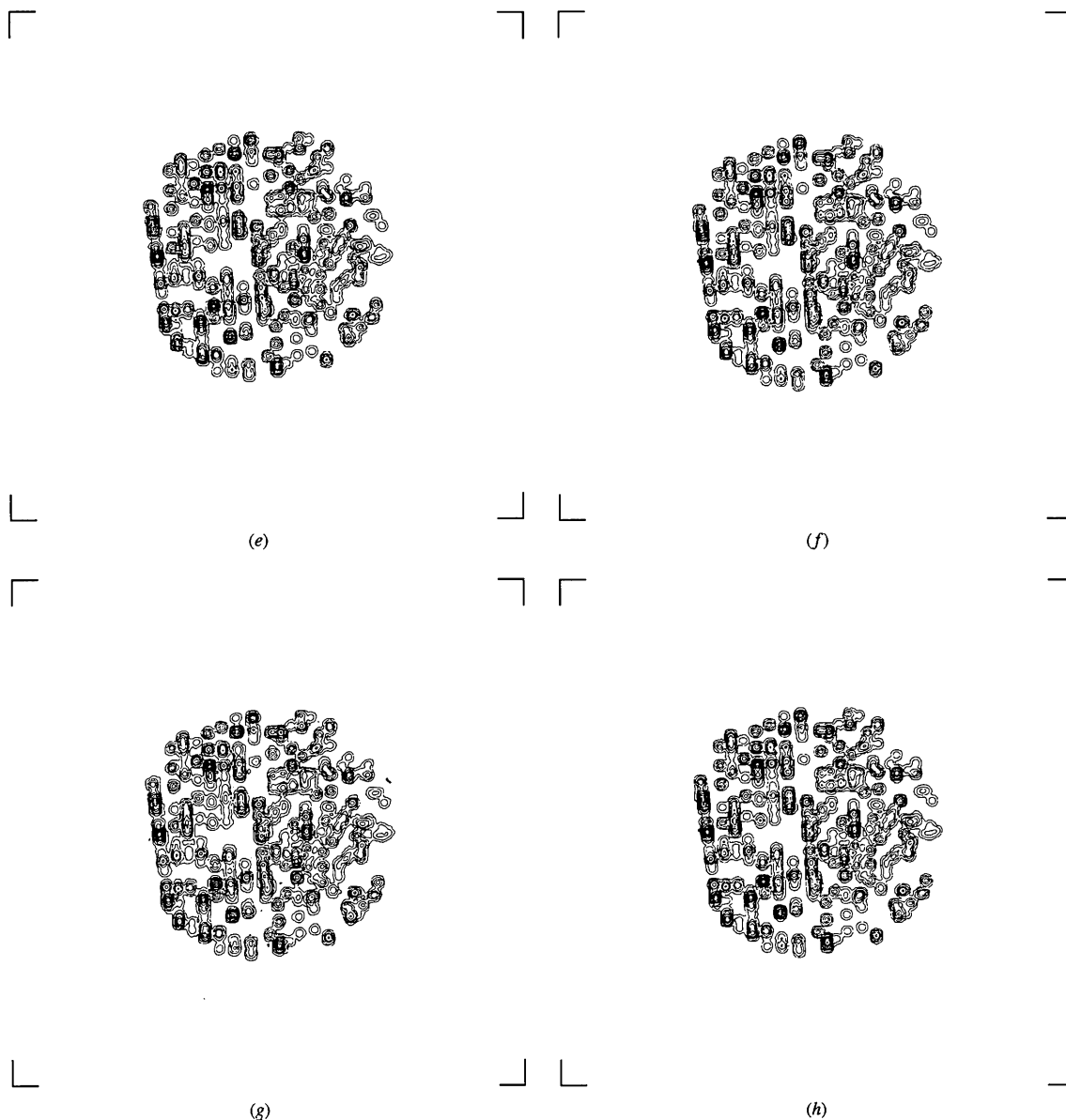
(e)

(f)

(g)

(h)

Fig. 4 (cont.)

Turning to the pattern as a whole, the intensity $|F(H, K, L)|^2$ of the pattern is continuous in H, K, L in the noncrystal case, where (H, K, L) is the continuous positional coordinate in reciprocal space. At the origin, $F(0, 0, 0)$ equals the number of electrons in the specimen. Moving away from the origin, $|F(H, K, L)|^2$ initially is high but is also rapidly decreasing, in keeping with the fact that the resolution elements, while initially large and hence containing large numbers of electrons scattering in phase, rapidly become smaller and less capable of strong scattering. Observability of the pattern terminates at the resolution where this resolution-element-size mechanism for coherency gain is no longer sufficient to counteract the effects of radiation damage in the specimen (Sayre & Chapman, 1995). Typically, as noted above, this occurs at approximately the same point where, in the crystal case, the Bragg mechanism, which at integral H, K, L provides enormous coherency gain equal to the number of unit cells in the crystal, first appears with large-unit-cell crystals. With this powerful gain mechanism available, visibility is greatly extended in crystallography to the entire extensive Bragg pattern, but in the noncrystal case this mechanism does not exist.

3. Phasing the pattern

The major remaining question about the concept concerns the phase problem. To discuss this, it may be noted that there are two losses of information that occur in a crystal diffraction experiment: one is the familiar fact that intensities but not phases are measured; the other is that intensities are measured at but not between the Bragg peaks. Following various partial ideas on the second of these (Boyes-Watson et al., 1947; Sayre, 1952; Bruck & Sodin, 1979), it was proved by Bates (1982) and Hayes (1982) that, if the intensities could be measured not only at the integral values corresponding to the Bragg peaks but also at the half-integral values, there would be enough information present to cause the phases also to be uniquely determined. The technique is somewhat related to solvent flattening in the crystal case. Applied to the present concept, this important result suggests that the continuous nature of the Fourier transform of noncrystal-line structures, while adding to the practical difficulty of observing the transform, may also provide the necessary method for phasing it.

To test this, a simulated two-dimensional oversampled data set was generated by computing the Fourier transform of a structure consisting of 500 circular real Gaussian scatterers distributed semirandomly and non-symmetrically within a circular support envelope of 1 μm diameter and outputting values of the magnitude of the transform on a square sampling lattice twice as fine as the Bragg lattice corresponding to repeating the structure with contact but without overlap; i.e. with 2× over-sampling in each dimension or 4× overall compared to what would be observed in the crystal case. The

scatterers had a diameter at half-maximum of 398 Å and the data set extended to a resolution of 300 Å. Care was taken to use the Fourier transform in this computation not the discrete Fourier transform, which would produce aliasing effects that are not encountered in real diffraction experiments.

This data set was then submitted to a phasing algorithm of the Bates/Hayes type, adapted from Fienup (1982), which starts with randomly assigned phases in reciprocal space, employs the discrete Fourier transform to iterate between real and reciprocal space, and applies constraints to the functions in the two spaces. The functions in both spaces were treated as complex, and no symmetry (e.g. Hermitian symmetry in reciprocal space) was imposed. The constraints employed were as follows: in reciprocal space, magnitudes were made equal to the supplied magnitudes; in direct space, outside the envelope, magnitudes were reduced towards zero and, inside the envelope, magnitudes were reduced towards zero if the real part was negative. Fig. 4 shows that essentially perfect reconstruction was achieved with error-free data and that reasonable noise in the data was well tolerated. Similar results have been obtained with other test structures and also with less than 2× oversampling in each dimension; in addition, a little work performed with three-dimensional data supports the expectation that such data will phase at least as readily as two-dimensional data. Altogether, except possibly for the effects of the difficulty of obtaining good values of $|F|$ close to and at the origin (the beam-stop effect), no problem areas have as yet been revealed. See Miao et al. (1998) for a fuller report on this work.

Before leaving the subject of phasing in the noncrystal case, it may be noted that the Bates/Hayes theorem is not the only possible approach in the noncrystalline case: another is direct physical phasing through the provision of a reference wave, i.e. X-ray holography (Lindaas et al., 1996); and a second is a recent technique involving both scanning and diffraction, introduced by Rodenburg & Bates (1992); brief descriptions of both are given in Sayre & Chapman (1995). A third possibility consists in placing a known crystal structure in close proximity to the unknown structure and collecting oversampled intensity data from this composite structure. If the crystal part makes up more than 50% of the composite and has a simple structure, a recent paper by Xu (1996) gives a method for solving the resulting Patterson map for the unknown structure. A periodic array of 100 Å gold spheres, if one could be fabricated, could serve as the known crystal for large biological structures.

4. Additional potentialities of the technique

§§2 and 3 of this paper have been concerned with answering the two principal questions concerning the feasibility of the concept under discussion: can the diffraction patterns be observed, and can they be phased?

The present section, on the other hand, briefly remarks on two potentialities of the concept that were mentioned earlier. These have to do with the use of soft-X-ray absorption-edge phenomena to increase the information that can be obtained from the specimen and the range of specimens that can be studied.

As discussed in §2, the noncrystal technique can be carried out in the soft-X-ray region of the spectrum, in which are found the inner-shell absorption edges of the low-Z atoms that principally make up biological matter. This has the effect of allowing it to produce maps not only of the structure of such specimens but of aspects of their chemistry as well. The process would consist in generating electron-density images at several X-ray wavelengths and inferring the chemistry at each map position by the manner in which the density there varies with wavelength, the presence of particular atomic species being indicated by sudden large density changes at absorption-edge wavelengths and the information about bonding and chemical state by smaller near-edge density variations. For a fuller discussion, the reader is referred to Kirz et al. (1995).

In addition, the large edge variations can be used to expand the range of specimens which can be imaged. An example is the imaging of hydrated, and therefore if desired initially living, biological cells; by working at wavelengths just above the oxygen-edge wavelength at 23 Å, a point can be obtained where the water in a specimen is weakly scattering, allowing the non-water structure to be imaged even in a hydrated specimen. More generally, by taking advantage of the scattering-factor variations available, investigators can arrange for a large variety of informative imaging possibilities, either with specimens in their natural state or with specimens with added labels or other constituents.

5. Conclusions

Evidence has been presented that, assuming further development of the techniques employed, a very large increase in the applicability of the X-ray crystallographic method can be realised, which would allow micrometer-size-range structures to be imaged without the need for incorporating them in crystals. Compared to the crystal case, there would be a large absolute loss of resolution but resolution relative to structure size would be essentially unchanged (Fig. 3). Benefits, in addition to those of much larger structure size and simplified specimen preparation, would include a direct technique of phasing, a potential for obtaining spatially resolved chemical information and the ability to image structures in a wide variety of states.

References

Bates, R. H. T. (1982). Optik (Stuttgart), 61, 247–262.
Boyes-Watson, J., Davidson, K. & Perutz, M. F. (1947). Proc. R. Soc. London Ser. A, 191, 83–132.
Bruck, Yu. M. & Sodin, L. G. (1979). Optic. Commun. 30, 304–308.
Fienup, J. R. (1982). Appl. Opt. 21, 2758–2769.
Guttmann, G. D., Henke, B. L. & Kerner, J. A. (1988). X-ray Microscopy II, edited by D. Sayre, M. Howells, J. Kirz & H. Rarback, pp. 151–153. Springer Series in Optical Sciences, Vol. 56. Berlin: Springer.
Hayes, M. H. (1982). IEEE Trans. Acoust. Speech Signal Process. 30, 140–154.
Kirz, J., Jacobsen, C. & Howells, M. (1995). Q. Rev. Biophys. 28(1), 33–130.
Lindaas, S., Howells, M., Jacobsen, C. & Kalinovsky, A. (1996). J. Opt. Sci. Am. A13, 1788–1800.
Miao, J., Sayre, D. & Chapman, H. N. (1998). J. Opt. Soc. Am. A. In the press.
Rarback, H., Buckley, C., Ade, H., Camilo, F., DiGennaro, R., Hellman, S., Howells, M., Iskander, N., Jacobsen, C., Kirz, J., Krinsky, S., Lindaas, S., McNulty, I., Oversluizen, M., Rothman, S., Sayre, D., Sharnoff, M. & Shu, D. (1990). J. X-ray Sci. Technol. 2, 274–296.
Rodenburg, J. M. & Bates, R. H. T. (1992). Philos. Trans. R. Soc. London Ser. A, 339, 521–553.
Sayre, D. (1952). Acta Cryst. 5, 843.
Sayre, D. (1980). Imaging Processes and Coherence in Physics, edited by M. Schlenker, M. Fimk, J. P. Goedgebuer, C. Malgrange, J. Ch. Viénot & R. H. Wade, pp. 229–235. Lecture Notes in Physics, Vol. 112. Berlin: Springer.
Sayre, D. (1991). Direct Methods of Solving Crystal Structures, edited by H. Schenk, pp. 353–356. NATO ASI Series B (Physics), Vol. 274. New York: Plenum.
Sayre, D. & Chapman, H. N. (1995). Acta Cryst. A51, 237–252; erratum: (1995), A51, 810.
Sayre, D., Haelbich, R. P., Kirz, J. & Yun, W. B. (1984). X-ray Microscopy, edited by G. Schmahl & D. Rudolph, pp. 314–316. Springer Series in Optical Sciences, Vol. 43. Berlin: Springer.
Sayre, D., Yun, W. B. & Kirz, J. (1988). X-ray Microscopy II, edited by D. Sayre, M. Howells, J. Kirz & H. Rarback, pp. 272–275. Springer Series in Optical Sciences, Vol. 56. Berlin: Springer.
Winick, H. (1994). Nucl. Instrum. Methods, B87, 112–115.
Xu, G. (1996). Appl. Phys. Lett. 68, 1901–1903.
Yun, W. B., Kirz, J. & Sayre, D. (1987). Acta Cryst. A43, 131–133.